Advances in Radiation Oncology (2023) 8, 101226

advances in radiation oncology

www.advancesradonc.org

Scientific Article

Prospective In Silico Evaluation of Cone-Beam Computed Tomography-Guided StereoTactic Adaptive Radiation Therapy (CT-STAR) for the Ablative Treatment of Ultracentral Thoracic Disease

Joshua P. Schiff, MD,[a,1] Eric Laugeman, MS,[a,1] Hayley B. Stowe, MD, MSCI,[a] Xiaodong Zhao, PhD,[a] Jessica Hilliard, BS,[a] Ellie Hawk, BS,[a] Jesiah Watkins, BS,[a] Casey Hatscher, BS,[a] Shahed N. Badiyan, MD,[a] Pamela P. Samson, MD, MPHS,[a] Geoffrey D. Hugo, PhD,[a] Clifford G. Robinson, MD,[a] Alex T. Price, MS,[b] and Lauren E. Henke, MD, MSCI[b,*]

[a]*Department of Radiation Oncology, Washington University School of Medicine in St Louis, St Louis, Missouri; and*
[b]*Department of Radiation Oncology, University Hospitals/Case Western Reserve University, Cleveland, Ohio*

Received 27 December 2022; accepted 15 March 2023

Abstract

Purpose: We conducted a prospective, in silico study to evaluate the feasibility of cone-beam computed tomography (CBCT)-guided stereotactic adaptive radiation therapy (CT-STAR) for the treatment of ultracentral thoracic cancers (NCT04008537). We hypothesized that CT-STAR would reduce dose to organs at risk (OARs) compared with nonadaptive stereotactic body radiation therapy (SBRT) while maintaining adequate tumor coverage.

Methods and Materials: Patients who were already receiving radiation therapy for ultracentral thoracic malignancies underwent 5 additional daily CBCTs on the ETHOS system as part of a prospective imaging study. These were used to simulate CT-STAR, in silico. Initial, nonadaptive plans (P_I) were created based on simulation images and simulated adaptive plans (P_A) were based on study CBCTs. 55 Gy/5 fractions was prescribed, with OAR constraint prioritization over PTV coverage under a strict isotoxicity approach. P_I were applied to patients' anatomy of the day and compared with daily P_A using dose-volume histogram metrics, with selection of superior plans for simulated delivery. Feasibility

Sources of support: This study was supported by Varian Medical Systems.

Joshua Schiff receives grants from Varian Medical Systems. Eric Laugeman has no disclosures. Hayley B Stowe has no disclosures. Xiaodong Zhao has no disclosures. Jessica Hillard has no disclosures. Ellie Hawk has no disclosures. Jesiah Watkins has no disclosures. Casey Hatscher has no disclosures. Shahed Badiyan receives honoraria from Mevion. Pamela Samson receives grants from Varian Medical Systems. Geoffrey Hugo receives grants from Varian Medical Systems, Siemens Healthineers, ViewRay, and Mevion, and royalties and consulting fees from Varian Medical Systems. Clifford Robinson receives research funding from Varian Medical Systems and Merck, leadership for Radialogica, stock for Radialogica, consulting for Varian Medical Systems, Astrazeneca, EMD Serono, Quantaras, and has US patent No. 62/598 and WO 2017078757. Alex Price receives grants from Varian Medical Systems and support for travel from ViewRay Inc and Sun Nuclear Corporation. Lauren Henke receives grants from Varian Medical Systems, consulting fees from Varian Medical Systems and Radialogica, honoraria from ViewRay, Varian Medical Systems, and LusoPalex, and participates on a safety board for ViewRay.

Research data are stored in an institutional repository and will be shared upon request to the corresponding author.

[1] J. P. Schiff and E. Laugeman contributed equally to this work and should be denoted as cofirst authors.

*Corresponding author: Lauren Henke, MD, MSCI; E-mail: lauren.henke@uhhospitals.org

https://doi.org/10.1016/j.adro.2023.101226

was defined as completion of the end-to-end adaptive workflow while meeting strict OAR constraints in ≥80% of fractions. CT-STAR was performed under time pressures to mimic clinical adaptive processes.

Results: Seven patients were accrued, 6 with intraparenchymal tumors and 1 with a subcarinal lymph node. CT-STAR was feasible in 34 of 35 simulated fractions. In total, 32 dose constraint violations occurred when the P_I was applied to anatomy-of-the-day across 22 of 35 fractions. These violations were resolved by the P_A in all but one fraction, in which the proximal bronchial tree dose was still numerically improved through adaptation. The mean difference between the planning target volume and gross total volume V100% in the P_I and the P_A was −0.24% (−10.40 to 9.90) and −0.62% (−11.00 to 8.00), respectively. Mean end-to-end workflow time was 28.21 minutes (18.02-50.97).

Conclusions: CT-STAR widened the dosimetric therapeutic index of ultracentral thorax SBRT compared with nonadaptive SBRT. A phase 1 protocol is underway to evaluate the safety of this paradigm for patients with ultracentral early-stage NSCLC.

Introduction

Although stereotactic body radiation therapy (SBRT) has become standard of care for medically inoperable early-stage non−small cell lung cancer (NSCLC) as well as an option for regionally recurrent or oligometastatic thoracic disease, the use of SBRT for the treatment of ultracentral thoracic disease remains controversial.[1-3] Several seminal clinical trials have established that the delivery of ablative doses of ultrahypofractionated radiation therapy to the ultracentral thorax, which may be defined as disease within 1 cm or touching the proximal bronchial tree, pulmonary arteries, and/or esophagus, can incur unacceptably high rates of grades 3 to 5 toxicity.[4-8] Most recently, the HILUS trial, in which 56 Gy in 8 fractions was delivered to tumors within 1 cm of the bronchial tree, demonstrated significant toxicity, with 34% and 15% of patients experiencing a grade 3 to 5 or grade 5 toxicity, respectively.[6] Given the concern for toxicity, many practitioners use more protracted radiation therapy regimens (60 Gy in 8-15 fractions). Although extended fractionation aims to mitigate risk to organs at risk (OARs), toxicity persists with these regimens, and they are often of subablative biologic effective doses (BED10 < 100 Gy) compared with typical SBRT regimens delivered in 5 or fewer fractions.[9-12]

Online adaptive radiation therapy (online ART) enhances the therapeutic ratio of SBRT by improving interfraction motion management via the use of daily recontouring and replanning to match a patient's anatomy of the day while the patient remains on the treatment table. Stereotactic magnetic resonance-guided adaptive radiation therapy (SMART) has been demonstrated to improve the dosimetric therapeutic index of SBRT and yield durable local control and toxicity in a variety of disease sites.[13-16] The dosimetric benefits of SMART as well as efficacy and toxicity have been demonstrated in thoracic disease, specifically with regards to central and ultracentral tumors.[17-21] In a large series by Finazzi et al,[19] 50 patients with high-risk lung tumors, including 29 patients with primary lung cancer, were treated with SMART. In this series, the local control at 12 months was 95.60% and there were no grade 4 or 5 toxicities. SMART for central and ultracentral early-stage NSCLC is currently being evaluated in a phase 2 prospective trial (NCT04917224) but is necessarily limited to the few centers with magnetic resonance imaging −guided radiation therapy.

Recently, a ring gantry computed tomography (CT)-guided linear accelerator (ETHOS; Varian Medical Systems, Palo Alto, CA) has become commercially available, enabling rapid acquisition of high-quality volumetric on-board cone-beam CT (CBCT) images. This imaging unit is coupled with a dedicated, on-board treatment planning system (TPS) capable of online ART.[22-24] Its utility for adaptive SBRT for the ultracentral thorax has yet to be investigated. In that context, we conducted a prospective in silico imaging clinical trial to evaluate the feasibility and potential dosimetric advantages of CBCT-guided stereotactic adaptive radiation therapy (CT-STAR) for the ablation of ultracentral thoracic disease.

Methods and Materials

Patients

Patients with ultracentral thoracic disease intended to be treated with standard-of-care external beam radiation therapy were enrolled in a prospective in silico trial between January 1, 2019, and February 15, 2022. Patients were mandated to be able to give informed consented, to be ≥18 years of age, and had either primary lung, locoregionally recurrent, or oligometastatic disease of the ultracentral thorax. Standard-of-care radiation therapy occurred in parallel with image acquisition for this study; clinical care took place on varying treatment machines in our department as delineated by the treating radiation oncologist and was not a focus of this study. The prospective clinical trial (NCT04008537) was approved by the institutional review board (Human Resource Protection Office #201908024).

Acquisition of imaging

Patients underwent 5 separate imaging sessions using ETHOS (v.02.01.00) kilovoltage CBCTs on 5 separate days to

capture interfraction motion. The images were obtained in end-exhale breath-hold, which is our institution's standard treatment position for thoracic SBRT on the ETHOS system, or deep-inhale breath-hold if the patient couldn't tolerate end-exhale breath-hold. These imaging sessions were scheduled at the convenience of the patient and preceded or followed their standard clinical radiation. A minimum of 1 CBCT scan was acquired per session. The protocol mandated that no more than 6 CBCT scans could be acquired per session and no more than 10 sessions in total. These images were then used to emulate, in silico, the online ART workflow. Patients were evaluated for adverse events possible related to study imaging, and further assessment was performed at on-treatment-visits and posttreatment follow-up.

Initial planning

Baseline treatment plans with the emulated prescription dose (55 Gy in 5 fractions [BED10 = 115.5Gy]) independent from their standard-of-care radiation therapy treatment plans were produced for all patients according to the patient's initial anatomy at CT simulation (P_I). Simulation typically consisted of a helical CT followed by a 4-dimensional CT. Intravenous contrast administration was dictated at the discretion of the treating physician. A custom immobilization device was used in which the patient was supine with both arms overhead, per our institutional thoracic SBRT policy. Gross tumor volume (GTV) was defined using simulation and diagnostic imaging, and no clinical target volume was used per standard institutional SBRT practice. An internal target volume was not defined as we were simulating treatment at breath-hold (our institutional standard for intrafraction motion management on ETHOS). The planning target volumes (PTV) comprised a standard 0.5-cm volumetric expansion of the GTVs.

The critical thoracic organs, namely trachea, proximal bronchial tree, great vessels, heart, esophagus, brachial plexus, and spinal cord were protected using a described, strict isotoxicity approach.[18] These OAR constraints may be reviewed in Table 1. As ultracentral tumors typically abut at least one of these names OARs, a planning optimization structure (PTV_{opt}) was used to direct target

Table 1 Constraint data and coverage metrics

Organ at risk	Constraint	No. of P_I constraint violations	P_I mean (range)	P_A mean (range)
Trachea	V50Gy <0.20cc	0	0.00 (0.00-0.00)	0.00 (0.00-0.00)
Proximal bronchial tree	V50Gy <0.20cc	22	0.74 (0.00-3.85)	0.08 (0.00 -0.92)
Great vessels	V47Gy <10.00cc	3	4.65 (0.00-14.79)	2.43 (0.05-6.98)
Heart	V32Gy <15.00cc	0	1.31 (0.00-4.63)	0.86 (0.00-3.61)
Esophagus	V32Gy <0.50cc	6	0.19 (0.00-1.88)	0.01 (0.00-0.10)
Stomach	V33Gy <0.50cc	0	0.00 (0.00-0.00)	0.00 (0.00-0.00)
Brachial plexus	V27Gy <3.00cc	0	0.02 (0.00-0.42)	0.01 (0.00-0.28)
Spinal cord	V25Gy <1.00cc	0	0.02 (0.00-0.35)	0.00 (0.00-0.01)
Chest wall*	V30Gy <30.00cc	1	13.31 (0.00-45.05)	11.64 (0.00-29.62)
Uninvolved lung*	CV12.5Gy <1500.00cc CV13.5Gy <1000.00cc	0	488.04 (277.75-992.44)	461.25 (277.75-992.44)
Target volume metric		Goal	P_I mean (range)	P_A mean (range)
PTV V100% (%)		N/A	80.67 (42.80-94.30)	80.43 (40.00-96.60)
PTV V50Gy (%)		N/A	86.96 (53.50-97.60)	87.16 (53.00-98.90)
PTV_{opt} D95% (Gy)		>95% Rx (10.45 Gy per fraction)	10.86 (8.20-11.61)	11.43 (10.77-11.82)
GTV V100% (%)		N/A	91.29 (65.60-99.90)	90.67 (63.40-100.00)
GTV V50Gy (%)		N/A	95.54 (76.50-100.00)	95.98 (79.10-100.00)
Planning metric		Goal	P_I mean (range)	P_A mean (range)
PTV CI		N/A	1.02 (0.48-1.26)	0.95 (0.42-1.26)
PTV_{opt} CI		N/A	1.33 (1.13-1.75)	1.24 (1.00-1.37)
PTV R50		N/A	3.85 (1.86-5.26)	3.54 (1.72-4.47)
PTV_{opt} R50		N/A	5.09 (4.38-7.57)	4.67 (4.24-5.29)

Abbreviations: CI = conformality index; CV = critical volume; GTV = gross total volume; N/A = not applicable; OAR = organ at risk; P_A = adapted plan; P_I = patient's initial anatomy at CT simulation; PTV = planning target volume.
OAR constraint data as well as coverage and planning metrics are demonstrated.
* Indicates an OAR constraint that is not a hard constraint, and therefore isn't a primary driver of tumor coverage.

coverage sacrifice in areas of PTV/OAR overlap. Creation of the PTV_{opt} structure is reviewed in Fig. 1. The optimization structure margin was 5 mm for esophagus, heart, brachial plexus, and 3 mm for trachea, bronchial tree, and great vessels. Notably, this structure is not specifically constrained (not a true planning organ at risk volume, or PRV) but is a tool for plan optimization to ensure prescription coverage of as much of the target as reasonably achievable while directing the dose fall-off region to meet strict OAR constraints for critical structures.

Adaptive planning

The ETHOS adaptive workflow has previously been described.[25-27] A vendor-supplied emulator (virtual workstation), which contains the same online ART TPS system as the clinical ETHOS system and allows the offline injection of previously acquired CBCT scans, was used to simulate online ART. Simulated online ART planning was timed and performed in concert by a physician and physicist to mirror the in vivo workflow. First, a CBCT scan was injected into the emulator. Then, the ETHOS integrated TPS generated "influencers" (critical OARs by disease site) via a pretrained, vendor-supplied convolutional neural network-based artificial intelligence auto-segmentation algorithm. In the ETHOS system, the right lung, left lung, and heart are thoracic "influencers." However, the artificial intelligence autosegmentation algorithm does not currently autosegment OARs in the thorax, and therefore all influencer contours were deformed onto the anatomy of the day in each simulated fraction and edited if needed in a latter workflow step. The planning-CT-defined GTV was then rigidly copied onto and aligned to the centroid of the GTV on the daily CBCT; our institution does not use the deformed GTV that is automatically generated by the TPS, as this does not account for critical diagnostic scan information used to delineate a GTV at time of simulation such as a CT with intravenous contrast or a positron emission tomography scan. GTV contours were edited at the discretion of the treating radiation oncologist and medical physicist if there was substantial tumor change or changes in patient alignment. All other OARs were automatically deformed from the planning CT to the injected CBCT. The GTV as well as OARs within a 3-cm contour ring (previously described for online ART planning[28]) were subsequently edited manually based on the patient's anatomy of the day and confirmed by the radiation oncologist. Edited contours were then used to create an adapted plan (P_A).

PTV coverage goals were the same for P_I and the P_A, again using a described strict isotoxicity approach. Each daily adapted fraction was planned and analyzed using a target dose and OAR constraint correlating with a 5-fraction regimen. The P_I was evaluated on the patient's anatomy of the day while the reoptimized P_A was generated. The P_I and P_A were then compared using dose volume histogram objectives, and the superior plan was delivered. The P_A was considered superior if it resolved ≥1 OAR hard constraints and/or improved target coverage by ≥5%.

Dosimetry and feasibility evaluation

Doses delivered to the PTV, PTV_{opt}, and GTV as well as the OARs in both the P_I and P_A were evaluated for each

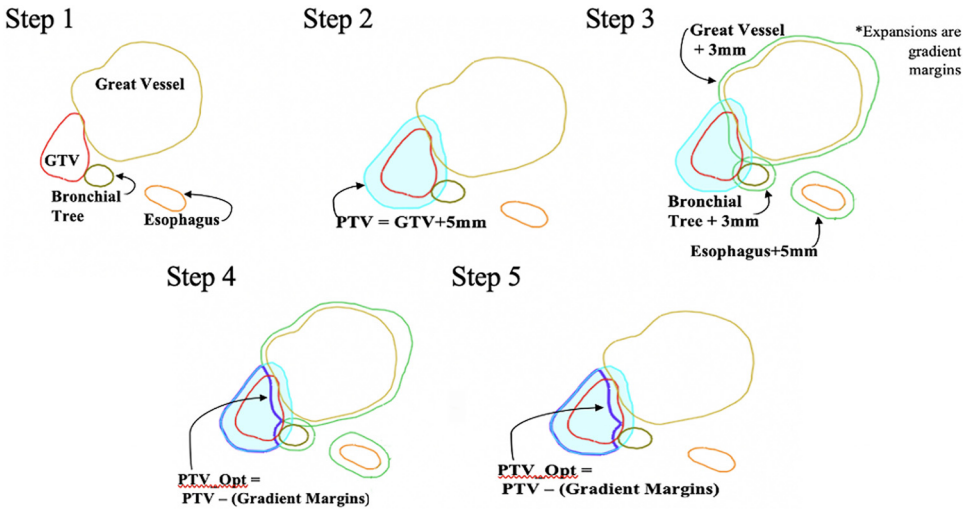

Figure 1 Creation of PTV_{opt} structure. This figure illustrates the steps necessary to creating the PTV_{opt} structure that dose is prescribed to. The PTV is generated using a 5-mm volumetric expansion of the GTV (Step 2). Gradient margins are created in Step 3, which are volumetric expansions of critical OARs. Finally, in Steps 4 and 5, the PTV_{opt} structure is created, which is the PTV minus the gradient margins. The PTV_{opt} structure is commonly used to prescribe dose to in standard adaptive radiation therapy practice and allows for de-escalation of dose at the interface of targets and critical OARs. *Abbreviations*: GTV = gross tumor volume; OAR = organ at risk; PTV = planning target volume.

fraction. Relevant planning metrics for thoracic SBRT including the conformality index and R50 were also evaluated. The conformality index was defined as the volume receiving 100% or greater of prescription dose divided by the target volume and the R50 was defined as the volume receiving 50% or greater of prescription dose divided by the target volume. The primary objective of this study was to demonstrate that a CT-STAR workflow was feasible for clinical use, which was defined as successful completion of online-ART with compliance with strict OAR constraints in ≥ 80% of simulated adaptive fractions.

Data collection and statistics

Baseline and treatment characteristics were collected on all patients enrolled in the study. Time points collected prospectively for each fraction of simulated CT-STAR have previously been described and are summarized in Table 2. Monitor units delivered were collected for each adapted fraction as well for the simulation (reference) fractions.

Results

Seven patients with ultracentral thoracic disease receiving standard of care radiation therapy were accrued to this prospective clinical imaging trial. Four of 7 patients had primary lung cancer, and 3 of 7 patients had locoregionally recurrent lung cancer. Six of 7 lesions were intraparenchymal. One lesion was a subcarinal lymph node. CT-STAR was feasible in 34 of 35 (97%) fractions, in silico, for the ablative treatment of ultracentral thoracic disease. Dosimetry results for the P_I and P_A are demonstrated in Table 1 and visualized in Figs. 2 and 3. There was a total of 32 dose constraint violations in the P_I which occurred across 22 of 35 (63%) fractions. Online adaptation was able to resolve a constraint violation in the P_I in all but one fraction. In that fraction, the V50Gy for the proximal bronchial tree in the P_I was 1.37 cc, which was numerically reduced to 0.92 cc in the P_A yet remained above the 0.20 cc constraint. In this patient, the bronchiole intended to be spared was located within the tumor, with the tumor wrapping around the bronchiole. After this fraction, we amended our planning template to further prioritize the bronchial tree to account for these challenging anatomic situations. Figure 4 demonstrates how daily online adaptation was able to resolve an OAR hard constraint violation in the P_I in the P_A when replanning based on the patient's anatomy-of-the-day.

Coverage metrics are demonstrated in Table 1 and visualized in Fig. 3. The mean difference between the PTV and GTV V100%Rx in the P_I and the P_A was −0.24% (−10.40 to 9.90) and −0.62% (−11.00 to 8.00), respectively. The mean difference between the PTV and GTV V50Gy in the P_I and the P_A was 0.20% (−5.40 to 7.50) and 0.44% (−5.60 to 7.80), respectively. The mean absolute difference between the PTV_{opt} D95Gy in the P_I and the P_A was 0.57 Gy (−0.04 to 3.23). Minimum

Table 2 Timing data

Time point	Mean time per fraction (range)	Description
Influencer creation	0.83 (0.50-1.12)	TPS deforms simulation heart and lung contours onto the patient's anatomy of the day
Influencer verification	0.35 (0.25-0.83)	Physician and physicist verify the deformed influencers
Target generation	1.07 (0.25-0.83)	TPS deforms GTV onto the patient's anatomy of the day
Target verification	1.82 (0.42-5.23)	Physicist rigidly copies the GTV over the deformed GTV and verifies its alignment
OAR and GTV contouring	13.60 (4.62-31.82)	Treating physician amends and/or recontours all OARs within the 3-cm contour ring as well as edits the GTV if needed
Plan generation	9.47 (6.97-11.88)	TPS generates the P_A while the P_I is simultaneously projected on the patient's anatomy of the day
Plan evaluation	1.19 (0.58-3.45)	The P_I and P_A are compared, and the superior plan is delivered. The P_A is selected if it resolves ≥1 OAR hard constraint violation and/or improves target coverage by ≥5%
Total	28.21 (18.02-50.97)	Total ETHOS adaptive workflow time

Abbreviations: GTV = gross total volume; N/A = not applicable; OAR = organ at risk; P_A = adapted plan; P_I = patient's initial anatomy at CT simulation; PTV = planning target volume; TPS = treatment planning system.
Average timing data per fraction are presented in minutes for each step of the workflow as well as the total workflow time. Included are descriptions of each step of the ETHOS adaptive workflow. Notably, the in silico workflow does not capture timing data while the patient is on the treatment table as well as timing data for intrafraction motion management via breath-hold. Timing data are presented in minutes.

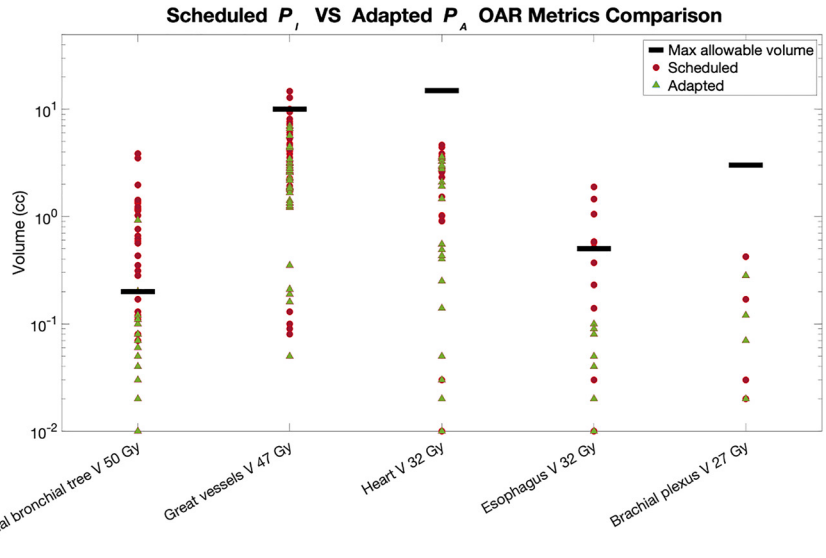

Figure 2 Computed tomography–guided stereotactic adaptive radiation therapy and nonadaptive OAR metrics. Hard constraint OAR metrics are demonstrated for both the scheduled (P_I) and adapted (P_A) plans. The adapted plans (green) only exceeded an OAR constraint (black) once, whereas the scheduled plans (red) exceeded a constraint 32 times. Data points in which the value was zero were excluded from this figure. The y-axis is log-scaled and the specific constraint data for each OAR can be reviewed in Table 1. *Abbreviation*: OAR = organ at risk.

coverage of 98% of the GTV was also evaluated, with the D98% being 9.82 Gy (5.42-11.67) in the P_I and 9.96 Gy (6.81-12.17) in the P_A. When evaluating the 6 intraparenchymal lesions alone, mean PTV V100%Rx was 86.89% (73.20-94.30) and 86.48% (62.8-96.6) in the P_I and P_A, respectively, and mean GTV V100%Rx was 95.42% (88.10-99.90) and 94.37 (77.10-100.00) in the P_I and P_A, respectively. Mean PTV V50Gy in those 6 patients was 92.44% (84.20-97.60) and 92.37% (80.10-89.90) in the P_I and P_A, respectively, and mean GTV V50Gy was 98.51% (94.50-100.00) and 98.33% (94.50-100.00) in the P_I and P_A, respectively.

Across all fractions, 1 or more coverage metrics were improved by at least 5% in 9 of 35 (26%) fractions, all of

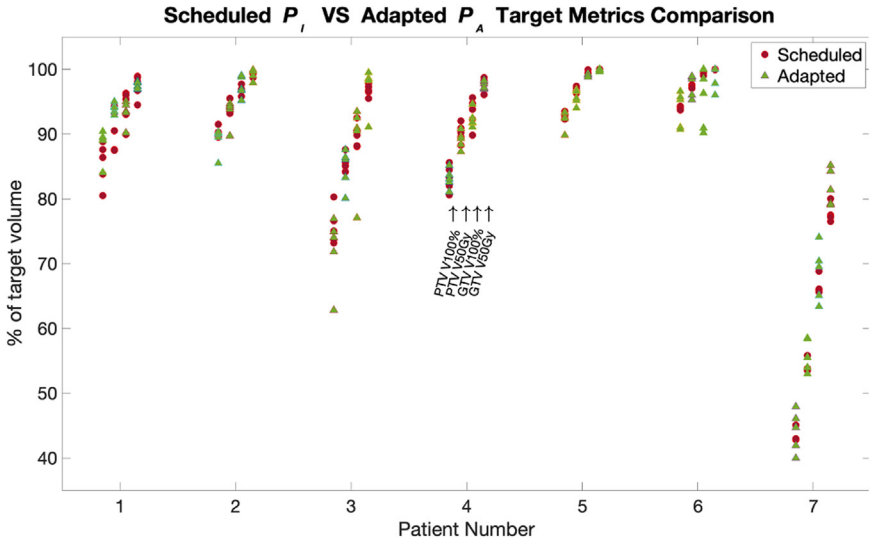

Figure 3 Computed tomography–guided stereotactic adaptive radiation therapy and nonadaptive target metrics. Coverage metrics are demonstrated for both the scheduled (P_I, red) and adapted (P_A, green) plans for each of the 7 patients on this clinical imaging study. Metrics presented from right to left per patients are PTV V100%, PTV V50Gy, GTV V100%, and GTV V50Gy. Patients one through 6 had intraparenchymal tumors, and patient 7 had a subcarinal lymph node. The specific data for each coverage metric can be reviewed in Table 1. *Abbreviations*: GTV = gross tumor volume; PTV = planning target volume.

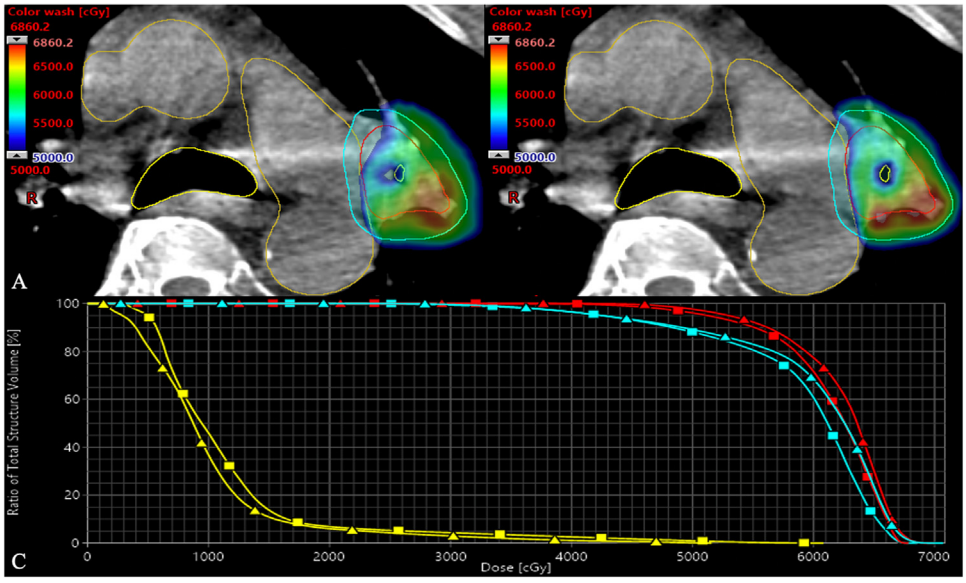

Figure 4 Computed tomography–guided stereotactic adaptive radiation therapy and nonadaptive plans. In this plan, which is projected on an ETHOS kv CBCT, a part of the proximal bronchial tree (yellow) is within the tumor, which can introduce significant challenge when treating ultracentral thoracic disease with SBRT. Here, minor changes in anatomy and rotation between simulation and treatment would have led to overdosing (≥50 Gy) of the proximal bronchial tree in the P_I (A) which was resolved in the P_A (B), all while maintaining GTV (red) and PTV (cyan) coverage. The dose to proximal bronchial tree, GTV, and PTV are represented in the DVH for both the P_I (squares) and P_A (triangles). *Abbreviations*: CBCT = cone-beam computed tomography; DVH = dose-volume histogram; GTV = gross tumor volume; PTV = planning target volume; SBRT = stereotactic body radiation therapy.

which were fractions in which 1 or more OAR constraint violation was resolved in the P_A. If this were a clinical cohort, 22 of 35 (63%) of the P_A would have been selected over the P_I, 13 of 35 (37%) for resolution of an OAR constraint violation, and 9 of 35 (26%) for our standard clinical criteria of adapting: (1) resolution of a strict OAR constraint violation and/or (2) improvement of target coverage by 5% or greater. In the remaining 13 of 35 (37%) of fractions, the P_I would have been considered acceptable for delivery by these institutional criteria. Timing data for this study are demonstrated in Table 2. Mean monitor units delivered in the reference and adapted plans were 5891.93 (4927.20-7331.30) and 5741.20 (4587.00-7331.30), respectively.

Discussion

We demonstrate here that CT-STAR widens the in silico dosimetric therapeutic index of SBRT for ultracentral thoracic disease and is a feasible treatment paradigm for this patient population. Adaptive replanning was able to resolve at least one OAR constraint violation in all but one fraction, and there were minimal average differences between GTV and PTV coverage in the P_I and the P_A. Although this study was performed to test this paradigm for all ultracentral thoracic tumors, special attention was paid to the 6 patients who were representative of patients who would be treated on a phase 1 protocol evaluating this paradigm for early NSCLC that is currently under development. In those 6 patients, PTV and GTV V100 coverage was markedly improved when excluding the theoretically nontrial eligible subcarinal lymph node patient, and the mean percent of volume of PTV and GTV receiving an effective ablative dose of radiation therapy (≥50 Gy/5 fractions = ≥100 Gy BED10) were greater than 90% and 95%, respectively, in both the P_I and the P_A.

The effective local control of early-stage NSCLC is generally thought to require a radiation therapy dose of BED10 ≥100 Gy for optimal outcomes, and yet the ablation of ultracentral lung tumors carries the inherent risk of incurring significant toxicities such as bronchovascular fistula or bronchopulmonary hemorrhage.[4,5,29,30] This excess toxicity was first described by Timmerman et al[4] in a series in which treatment of central lung tumors to 60 to 66 Gy/3fx resulted in greater rates of grade 3+ toxicity compared with treatment of peripheral lung tumors (27% vs 10%). The overall grade 5 treatment rate for this study was 7% for all patients. This toxicity risk has been replicated in multiple subsequent studies,[5-7] but most recently in the HILUS trial, in which patients with tumors ≤1 cm from the proximal bronchial tree were treated with 56 Gy/8 fractions.[6] Their analysis demonstrated that the maximum dose to 0.2 cc of the main bronchi and trachea was the strongest predictor of lethal bronchopulmonary hemorrhage, highlighting the paramount need to account

for maximum doses delivered to critical central thoracic OARs. The high toxicity demonstrated in these trials demonstrates that there is need for a technique such as the one developed, tested, and described within this study to widen the therapeutic index of SBRT for ultracentral thoracic disease. In this study, we demonstrate that CT-STAR was able to meet standard 5 fraction lung SBRT constraints in all but one fraction, suggesting that this technique may produce a more favorable toxicity profile than the one produced by previously tested ablative methods for the ultracentral thorax.

Because of the established concern and demonstrated risk of traditional ablative SBRT (5 or fewer fractions by United States definition) regimens, patients with ultracentral tumors are often treated with hypofractionated courses like 60 Gy in 8 to 15 fractions in our clinic. This is based on the theory that increasing fractionation reduces central thorax OAR risk and the data suggesting that these less ablative fractionation schemes are better tolerated.[5,9,10] For example, a series from the University of Kansas evaluating the treatment of ultracentral lung tumors with a 10-fraction regimen demonstrated limited grade 3 esophagitis and no grade 4 or 5 toxicities.[9] However, the 1-year local control rate in this study was 84%, less than what one would expect from a 5-fraction regimen. Therein lies the compromise and issue with many 8 to 15 fraction regimens, as these regimens typically have suboptimal BED10 (<100 Gy) for effective local control.[29] The BED10 of 60 Gy in 8, 10, 12, and 15 fractions is 105, 96, 90, and 84, respectively. Given the significant dose heterogeneity in SBRT planning and coverage compromises near OARs, it's possible that significant portions of a tumor could receive <100 Gy BED10, even in a 60-Gy-in-8-fraction regimen. Therefore, one may surmise that the development of an ablative technique capable of delivering a high BED10 (≥100 Gy) to the ultracentral thorax while respecting OAR hard constraints may be of significant benefit to this patient population. In this in silico study, CT-STAR was able to maintain the volume of PTV and GTV receiving ≥100 Gy BED10 to greater than 92% and 98%, respectively, for the patients with intraparenchymal tumors, suggesting that the technique may be able to ablate ultracentral thoracic disease without incurring significant toxicity.

The adaptive approach, including the sacrificing of coverage to prioritize strict OAR constraints while maximizing coverage in areas in which the PTV does not directly overlap with a critical OAR, is well studied in several disease sites. One disease site in which this methodology is well studied that has similarities to ultracentral NSCLC is pancreatic cancer. Like central and ultracentral NSCLC, local control may be improved with delivery of a radiation therapy dose of BED10 ≥100 Gy, which is challenging to deliver, given the proximity of adjacent critical OARs.[15,16,31-33] In addition, as in the treatment of ultracentral disease, the priority is to limit the max dose delivered to these critical OARs. Online-ART has been demonstrated to improve the therapeutic ratio of SBRT for pancreatic cancer, and our institution and others have demonstrated excellent local control and toxicity outcomes, as well as encouraging overall survival signals with this approach.[15] However, unlike pancreatic cancer, in which overall survival for even localized disease is quite poor, patients with early-stage ultracentral NSCLC have curable disease, and it may be of concern that tumors in otherwise-curable patients are underdosed using a PTV_{opt} approach. However, minimum tumor coverage was adequate in this in silico study, and both GTV and PTV coverage by at least 100 Gy BED10 were excellent in both the P_I and the P_A when excluding the patient with a nonintraparenchymal tumor. This also compares favorably to common clinical strategies used today, in which sacrifices of ablative dosing are knowingly made through subablative, hypofractionated approaches. Furthermore, in a future clinical implementation of CT-STAR, one could consider minimum GTV coverage metrics to optimally select patients for this approach, such as dose to 98% of the GTV needing to be ≥45.00 Gy (9.50 Gy per fraction), which is an equivalent dose by BED conversion to the BED10 of a 60 Gy in 12 fractions regimen typically offered, off-trial, for patients with ultracentral disease in our clinic. In this present study, the mean GTV D98% was 9.82 Gy (5.42-11.67) in the P_I and 9.96 Gy (6.81-12.17) in the P_A, which would meet that minimum coverage requirement and thus ensure that at least equivalent tumor ablation would be offered. For patients in whom these minimum coverage requirements cannot be achieved, it may be preferable to treat with standard, more protracted and nonadaptive regimens.

This in silico study has also yielded several important lessons that have been critical in the further development of this technique for future in vivo implementation. We have observed that when critical OARs, namely the proximal bronchial tree, bisect the tumor, it is particularly challenging to resolve OAR constraint violations through optimization alone. In fact, the sole fraction in this study where the TPS was unable to resolve this constraint violation was in this anatomic setting. Therefore, we have updated our ETHOS planning template to add additional optimization objectives to further prioritize the bronchial tree in these patients as well as permit the TPS to increase normalization, as needed, to meet this constraint in these challenging anatomic scenarios (Fig. 4). Another interesting point is that not all fractions required daily online adaptation, which is in contrast to upper abdominal adaptive SBRT literature, where nearly all fractions benefit dosimetrically from adaptive planning.[15,34] In our clinic, adaptation is used when an OAR strict constraint is resolved and/or when target coverage is improved by at least 5% in the adaptive plan. Applying those goals to this study, 63% percent of patients would have been adapted in this study. However, 6 of 7 patients benefitted, in silico,

from adaptation of at least 1 fraction, and it is logical that although thoracic OARs are somewhat mobile, there are fewer degrees of freedom to OAR motion in the central thorax compared with the upper abdomen.

Limitations of this study include the in silico design and small patient cohort. However, the small patient cohort was somewhat intentional, as it was determined by the clinical trials team that this was a reasonable number of patients to accrue to determine the dosimetric feasibility of CT-STAR for patients with ultracentral thoracic disease. Although timing data are comparable with previous in silico and in vivo adaptive data,[13,25,26] the adaptive sessions performed on the emulator in this trial were separate from the imaging sessions in which patients were physically on the table to maximize patient convenience. Therefore, the timing data might underestimate the time it takes for adaptation as well as treatment, particularly for patients treated at breath-hold. Although these data demonstrate that this paradigm is dosimetrically feasible in silico, confirmatory in vivo clinical data evaluating the use of CT-STAR for the ablative treatment of ultracentral thoracic disease are needed to evaluate the effect of this paradigm on the therapeutic index.

Conclusion

The data from this prospective in silico imaging clinical trial demonstrate the feasibility and dosimetric advantages of CT-STAR for the treatment of ultracentral thoracic disease. In this study, OAR hard constraints were resolved while maintaining adequate tumor coverage, a critical factor for a vulnerable yet curable patient population. A prospective protocol in which this paradigm will be evaluated in patients with ultracentral early-stage NSCLC in the clinic is currently open and accruing (NCT05785845).

References

1. Timmerman R, Paulus R, Galvin J, et al. Stereotactic body radiation therapy for inoperable early stage lung cancer. *JAMA*. 2010;303:1070-1076.
2. Timmerman R, Papiez L, McGarry R, et al. Extracranial stereotactic radioablation: Results of a phase I study in medically inoperable stage I non-small cell lung cancer. *Chest*. 2003;124:1946-1955.
3. Timmerman RD, Hu C, Michalski JM, et al. Long-term results of stereotactic body radiation therapy in medically inoperable stage I non–small cell lung cancer. *JAMA Oncol*. 2018;4:1287-1288.
4. Timmerman R, McGarry R, Yiannoutsos C, et al. Excessive toxicity when treating central tumors in a phase II study of stereotactic body radiation therapy for medically inoperable early-stage lung cancer. *J Clin Oncol*. 2006;24:4833-4839.
5. Tekatli H, Haasbeek N, Dahele M, et al. Outcomes of hypofractionated high-dose radiotherapy in poor-risk patients with "ultracentral" non-small cell lung cancer. *J Thorac Oncol*. 2016;11:1081-1089.
6. Lindberg K, Grozman V, Karlsson K, et al. The HILUS-trial—a prospective nordic multicenter phase 2 study of ultracentral lung tumors treated with stereotactic body radiotherapy. *J Thorac Oncol*. 2021;16:1200-1210.
7. Bezjak A, Paulus R, Gaspar LE, et al. Safety and efficacy of a five-fraction stereotactic body radiotherapy schedule for centrally located non-small-cell lung cancer: NRG Oncology/RTOG 0813 Trial. *J Clin Oncol*. 2019;37:1316-1325.
8. Haseltine JM, Rimner A, Gelblum DY, et al. Fatal complications after stereotactic body radiation therapy for central lung tumors abutting the proximal bronchial tree. *Pract Radiat Oncol*. 2016;6:e27-e33.
9. Sood SS, Shen X, Chen AM, Wang F. Ultracentral thoracic reirradiation using 10 fraction stereotactic body radiation therapy for recurrent non–small cell lung cancer tumors: preliminary toxicity and efficacy outcomes. *Int J Radiat Oncol Biol Phys*. 2017;99:E497.
10. Westover KD, Loo BW, Gerber DE, et al. Precision hypofractionated radiation therapy in poor performing patients with non-small cell lung cancer: Phase 1 dose escalation trial. *Int J Radiat Oncol Biol Phys*. 2015;93:72-81.
11. Lodeweges JE, van Rossum PSN, Bartels MMTJ, et al. Ultra-central lung tumors: Safety and efficacy of protracted stereotactic body radiotherapy. *Acta Oncol*. 2021;60:1061-1068.
12. Li Q, Swanick CW, Allen PK, et al. Stereotactic ablative radiotherapy (SABR) using 70 Gy in 10 fractions for non-small cell lung cancer: Exploration of clinical indications. *Radiother Oncol*. 2014;112:256-261.
13. Henke LE, Stanley JA, Robinson C, et al. Phase I trial of stereotactic MRI-guided online adaptive radiation therapy (SMART) for the treatment of oligometastatic ovarian cancer. *Int J Radiat Oncol Biol Phys*. 2022;112:379-389.
14. Henke L, Kashani R, Yang D, et al. Simulated online adaptive magnetic resonance-guided stereotactic body radiation therapy for the treatment of oligometastatic disease of the abdomen and central thorax: Characterization of Potential Advantages. *Int J Radiat Oncol Biol Phys*. 2016;96:1078-1086.
15. Hassanzadeh C, Rudra S, Bommireddy A, et al. Ablative five-fraction stereotactic body radiation therapy for inoperable pancreatic cancer using online MR-guided adaptation. *Adv Radiat Oncol*. 2021;6:100506.
16. Chuong MD, Bryant J, Mittauer KE, et al. Ablative 5-fraction stereotactic magnetic resonance-guided radiation therapy with on-table adaptive replanning and elective nodal irradiation for inoperable pancreas cancer. *Pract Radiat Oncol*. 2021;11:134-147.
17. Henke LE, Olsen JR, Contreras JA, et al. Stereotactic MR-guided online adaptive radiation therapy (SMART) for ultracentral thorax malignancies: Results of a phase 1 trial. *Adv Radiat Oncol*. 2019;4:201-209.
18. Henke LE, Kashani R, Hilliard J, et al. In silico trial of MR-guided midtreatment adaptive planning for hypofractionated stereotactic radiation therapy in centrally located thoracic tumors. *Int J Radiat Oncol Biol Phys*. 2018;102:987-995.
19. Finazzi T, Haasbeek CJA, Spoelstra FOB, et al. Clinical outcomes of stereotactic MR-guided adaptive radiation therapy for high-risk lung tumors. *Int J Radiat Oncol Biol Phys*. 2020;107:270-278.
20. Finazzi T, Palacios MA, Spoelstra FOB, et al. Role of on-table plan adaptation in MR-guided ablative radiation therapy for central lung tumors. *Int J Radiat Oncol Biol Phys*. 2019;104:933-941.
21. MRIdian® MRI-guided radiation therapy shows positive results in treatment of ultracentral/central lung tumors. Moffitt Cancer Center. Available at: https://moffitt.org/for-healthcare-professionals/clinical-perspectives/clinical-perspectives-story-archive/mridian-mri-guided-radiation-therapy-shows-positive-results-in-treatment-of-ultracentralcentral-lung-tumors/. Accessed October 11, 2022.
22. Hao Y, Cai B, Green O, et al. Technical Note: An alternative approach to verify 6FFF beam dosimetry for Ethos and MR Linac without using a 3D water tank. *Med Phys*. 2021;48:1533-1539.

23. Kim T, Ji Z, Lewis B, et al. Visually guided respiratory motion management for Ethos adaptive radiotherapy. *J Appl Clin Med Phys*. 2022;23:e13441.
24. Pokharel S, Pacheco A, Tanner S. Assessment of efficacy in automated plan generation for Varian Ethos intelligent optimization engine. *J Appl Clin Med Phys*. 2022;23:e13539.
25. Schiff JP, Price AT, Stowe HB, et al. Simulated computed tomography-guided stereotactic adaptive radiotherapy (CT-STAR) for the treatment of locally advanced pancreatic cancer. *Radiother Oncol J Eur Soc Ther Radiol Oncol*. 2022;175:144-151.
26. Schiff JP, Stowe HB, Price A, et al. In silico trial of computed tomography-guided stereotactic adaptive radiation therapy (CT-STAR) for the treatment of abdominal oligometastases. *Int J Radiat Oncol Biol Phys*. 2022;114:1022-1031.
27. Kim M, Schiff JP, Price A, et al. The first reported case of a patient with pancreatic cancer treated with cone beam computed tomography-guided stereotactic adaptive radiotherapy (CT-STAR). *Radiat Oncol Lond Engl*. 2022;17:157.
28. Bohoudi O, Bruynzeel AME, Senan S, et al. Fast and robust online adaptive planning in stereotactic MR-guided adaptive radiation therapy (SMART) for pancreatic cancer. *Radiother Oncol*. 2017;125:439-444.
29. Onishi H, Shirato H, Nagata Y, et al. Hypofractionated stereotactic radiotherapy (HypoFXSRT) for stage I non-small cell lung cancer: Updated results of 257 patients in a Japanese multi-institutional study. *J Thorac Oncol*. 2007;2(7 suppl 3):S94-100.
30. Onishi H, Shirato H, Nagata Y, et al. Stereotactic body radiotherapy (SBRT) for operable stage I non-small-cell lung cancer: Can SBRT be comparable to surgery? *Int J Radiat Oncol Biol Phys*. 2011;81:1352-1358.
31. Reyngold M, Parikh P, Crane CH. Ablative radiation therapy for locally advanced pancreatic cancer: Techniques and results. *Radiat Oncol Lond Engl*. 2019;14:95.
32. Chang DT, Schellenberg D, Shen J, et al. Stereotactic radiotherapy for unresectable adenocarcinoma of the pancreas. *Cancer*. 2009;115:665-672.
33. Krishnan S, Chadha AS, Suh Y, et al. Focal radiation therapy dose escalation improves overall survival in locally advanced pancreatic cancer patients receiving induction chemotherapy and consolidative chemoradiation. *Int J Radiat Oncol Biol Phys*. 2016;94:755-765.
34. Henke L, Kashani R, Robinson C, et al. Phase I trial of stereotactic MR-guided online adaptive radiation therapy (SMART) for the treatment of oligometastatic or unresectable primary malignancies of the abdomen. *Radiother Oncol J Eur Soc Ther Radiol Oncol*. 2018;126:519-526.